Research Article

Construction and Validation of Binary Phase Diagram for Amorphous Solid Dispersion Using Flory–Huggins Theory

Krishna Bansal,[1] Uttam Singh Baghel,[2] and Seema Thakral[1,3,4]

Abstract. Drug–polymer miscibility is one of the fundamental prerequisite for the successful design and development of amorphous solid dispersion formulation. The purpose of the present work is to provide an example of the theoretical estimation of drug–polymer miscibility and solubility on the basis of Flory–Huggins (F–H) theory and experimental validation of the phase diagram. The F–H interaction parameter, χ_{d-p}, of model system, aceclofenac and Soluplus, was estimated by two methods: by melting point depression of drug in presence of different polymer fractions and by Hildebrand and Scott solubility parameter calculations. The simplified relationship between the F–H interaction parameter and temperature was established. This enabled us to generate free energy of mixing (ΔG_{mix}) curves for varying drug–polymer compositions at different temperatures and finally the spinodal curve. The predicted behavior of the binary system was evaluated through X-ray diffraction, differential scanning calorimetry, and *in vitro* dissolution studies. The results suggest possibility of employing interaction parameter as preliminary tool for the estimation of drug–polymer miscibility.

KEY WORDS: amorphous solid dispersion; Flory–Huggins interaction parameter; miscibility; phase diagram; physical stability.

INTRODUCTION

Solubility and permeability are considered to be the two important biopharmaceutical properties, which together with potency ultimately determine the clinical efficacy of drug (1). It has been reported that ~70% of new chemical entities have poor aqueous solubility and consequently exhibit low oral bioavailability (2). Intensive academic as well as industrial research efforts have been targeted towards investigating approaches that can be used to improve aqueous solubility of such molecules. Some of the most widely used approaches used for the purpose include formation of prodrugs, complexation with the suitable host/complexing agent, salt formation (for weakly basic and acidic drugs), use of appropriate cosolvents or surfactants, and solid-state manipulation (which includes use of an appropriate polymorphs or reduction of particle size of drug). As the solid state of a drug is known to significantly affect the pharmaceutical properties, solid-state manipulation poses a viable avenue for solubility improvement and hence dissolution rate enhancement (3). A drug may exist either in an ordered crystalline form or in an amorphous form, where molecules lack lattice periodicity. The disorderliness in molecular arrangement bestows amorphous systems with excess thermodynamic properties (relative to the crystalline state) which contribute to higher solubility of the amorphous form (4,5). However, it also makes the amorphous form of the drug inherently unstable. As a result, the drug in the amorphous state may tend to crystallize either during storage and/or upon exposure to dissolution media. Such features often necessitate the incorporation of a polymeric excipient as a stabilizer for the amorphous drug, and the resulting drug–polymer binary system is presented in the form of a solid dispersion (SD) (6–9).

Numerous reports establish the effectiveness of polymer in the stabilization of amorphous drug (10). Recent studies are focused towards elucidation of the basic mechanisms by which such an effect is attained (11). For example, elevation of glass transition temperature (T_g) of amorphous drug by incorporation of high-T_g polymer has been shown to reduce molecular mobility (i.e., increased relaxation time) required for crystallization at a certain storage temperature (12). Specific intermolecular interactions between drug and polymer are also reported to stabilize the amorphous drug (13). Thermodynamic principles suggest reduction in chemical potential of drug on mixing with polymer, thus lowering the driving force for crystallization. It is also expected that a mutually miscible drug–polymer binary system will potentially stabilize the amorphous form of the drug.

Two components are generally considered to be miscible when their homogenous mixing at the molecular level is favored thermodynamically. Also, for a miscible drug–polymer system, it is expected that the drug stays in the supercooled liquid (liquid at temperature below the crystalline melting point T_m and above T_g) state without crystallization within

[1] GVM College of Pharmacy, Sonipat, Haryana 131001, India.
[2] Khalsa College of Pharmacy, Amritsar, Punjab 143001, India.
[3] College of Pharmacy, University of Minnesota, Minneapolis, Minnesota 55455, USA.
[4] To whom correspondence should be addressed. (e-mail: sthakral109@gmail.com)

the experimental time frame. As the amorphous drug is usually metastable relative to the crystalline state and may tend to crystallize, the system would eventually reach equilibrium with regard to the crystalline drug. The equilibrium composition of the mixture, in this case, would be the "solubility" of the crystalline drug in the polymer. The terms "solubility" and "miscibility" at temperatures close to and below T_g are considered to be "apparent" and estimated by extrapolation or model predictions (14). The present study investigates the use of well-established Flory–Huggins (F–H) theory (15,16) in estimation of drug–polymer miscibility and its significance in the successful design and development of a physically stable SD formulation.

F–H solution theory is an extension of the original regular solution theory and is extensively used for the estimation of free energy of mixing of polymer–solvent systems as well as polymer–polymer blends. The theory takes into consideration the non-ideal entropy of mixing of a large polymer molecule with small solvent molecules and the contribution due to the enthalpy of mixing. It has also been applied to describe the thermodynamics of drug–polymer system by considering amorphous drug molecules analogous to the solvent molecules. Hence the free energy of mixing for a drug–polymer system, ΔG_{mix} is described by

$$\frac{\Delta G_{mix}}{RT} = \varphi_d \ln \varphi_d + \frac{\varphi_p}{m} \ln \varphi_p + \chi_{d\text{-}p} \varphi_d \varphi_p \qquad (1)$$

where φ_d and φ_p denote the volume fraction of the drug and polymer, respectively; m is the ratio of the volume of a polymer chain to drug molecular volume, $\chi_{d\text{-}p}$ is known as the F–H interaction parameter for the particular drug–polymer system, R is the molar gas constant, and T is the temperature. The first two terms on the right-hand side of Eq. 1 estimate the entropy of mixing of a polymer and drug, whereas the last term including $\chi_{d\text{-}p}$ estimate the contribution from a non-zero enthalpy of mixing. As the configurational entropy always favors mixing for all combinations and compositions, it is the enthalpic component of ΔG_{mix} which determines whether or not mixing may be spontaneous. In the enthalpic component, the binary interaction parameter, $\chi_{d\text{-}p}$, is naturally expected to be critical for understanding as well as predicting the behavior of a drug–polymer binary system (13). A value of $\chi_{d\text{-}p} \leq 0$, indicative of adhesive interaction between drug and polymer molecules, would facilitate mixing. On the other hand, $\chi_{d\text{-}p} > 0$, indicative of strong cohesive forces either within the drug or within the polymer molecules, is expected to offset the entropic gain due to mixing.

Most of the established experimental methods for the determination of interaction parameter for the solvent–polymer systems (such as vapor pressure reduction, inverse gas chromatography, and osmotic pressure measurements) are not practically feasible for a drug–polymer binary system. Semi-empirical methods which have been used for the determination of $\chi_{d\text{-}p}$ include the following: (A) *a priori* estimates using solubility parameters (17–20) and (B) using melting point depression of drug in the presence of polymer for estimation of $\chi_{d\text{-}p}$ (21,22). In addition, molecular dynamic simulation and determination of solubility of drug in low-molecular weight analog of polymer have also been used for the estimation of the interaction parameter (13,23).

Recently, there has been emphasis on the realization that the interaction parameter $\chi_{d\text{-}p}$ is expected to vary with the temperature as well as the composition of the system (24,25). To incorporate temperature and composition dependence, $\chi_{d\text{-}p}$ is defined as

$$\chi_{d\text{-}p} = A + \frac{B}{T} + C_1 \varnothing + C_2 \varnothing^2 \qquad (2)$$

where A is the value of the temperature-independent term (entropic contribution), while B is the value of the temperature-dependent term (enthalpic contribution); C_1 and C_2 are fitting constants of $\chi_{d\text{-}p}$ with respect to composition of the system. Subsequently, the relationship has been simplified based on the assumption that the dependence of $\chi_{d\text{-}p}$ on the composition may be considered negligible relative to the effect of temperature and is represented as

$$\chi_{d\text{-}p} = A + \frac{B}{T} \qquad (3)$$

According to the Eq. 3, a decrease in temperature leads to corresponding increase in the value of interaction parameter. The interactions between molecules become increasingly less favorable to mixing and, at a given stage, a situation will be reached where the system will tend to phase separate into two different phases. It is possible to estimate the relationship between $\chi_{d\text{-}p}$ and T within a given temperature range for a drug–polymer binary systems. Thus, by combining Eq. 1 with Eq. 3, ΔG_{mix} *vs.* composition curves for a binary systems can be constructed for different temperatures. These curves can then be used to identify regions of stability, metastability, and instability for a particular system (14,23,26). The binodal curve separates the stable from the metastable regions of the phase diagram. It coincides with the set of points where the first derivative of the ΔG_{mix} curve with respect to composition is zero. The spinodal curve separates the metastable and unstable regions in the phase diagram. It corresponds to the inflection points where the relationship $\partial^2 \Delta G_{mix} / \partial \varphi_d^2 = 0$ holds. The spinodal curve can be easily estimated using Eq. 4.

$$\frac{1}{\varphi_d} + \frac{1}{m \varphi_p} - 2\chi_{d\text{-}p} = 0 \qquad (4)$$

Here, the value of interaction parameter $\chi_{d\text{-}p(s)}$ corresponding to spinodal at any temperature may be obtained from Eq. 3.

It is of theoretical as well as practical interest to construct temperature–composition phase diagram at fixed pressure and identify regions within the phase diagram where single-phase system is expected to be stable and regions where the binary system is expected to undergo phase separation into two phases. Though, in general, $\Delta G_{mix} < 0$ is the criteria for spontaneous mixing, it does not guarantee a single-phase system. Even for a homogenous single-phase binary system of composition possessing $\Delta G_{mix} < 0$, phase separation can occur if the system can lower its total free energy by dividing into two phases. Thus, as long as ΔG_{mix} *vs.* composition curve is concave up, phase separation would lead to increase free energy. "Concave up" can be considered as the criteria for stable single-phase system. Thus miscibility, in this context,

can be defined as the equilibrium composition of the two components, below which the free energy of mixing is less than zero and phase separation is thermodynamically not favorable (14).

Over the last decade, considerable progress has been made in the application of F–H theory to drug–polymer systems for the evaluation of thermodynamic parameters related to mixing of drug and polymer. Marsac *et al.* estimated values of the F–H interaction parameter for mixtures of nifedipine and indomethacin with poly vinyl pyrrolidine (PVP), with more negative values being observed with indomethacin, suggesting that indomethacin has a more negative enthalpy of mixing with PVP than nifedipine (22,23). These results were consistent with the observation that indomethacin forms stronger hydrogen bonds with the polymer than does nifedipine. F–H theory was used to predict the temperature–composition phase diagram of the model system indomethacin–PVP–VA and felodipine–PAA system (27,28). Small-scale thermal methods have been proposed that can be used in combination with F–H interaction theory to predict the physical stability of drug–polymer systems, e.g., HPMCAS-HF–felodipine and Soluplus–felodipine amorphous solid dispersions systems (26). The theoretical phase diagram of drug–polymer system has been evaluated by comparing experimentally determined solubility as well as miscibility of drug in polymer and the glass transition of the binary system (29).

The present study is based on estimation of $\chi_{d\text{-}p}$ using aceclofenac and Soluplus (a graft copolymer comprising of polyvinyl caprolactum–polyvinyl acetate-polyethylene glycol) as the model drug–polymer system. A representative phase diagram for the binary system was constructed using the estimated interaction parameter and was subsequently validated in a qualitative manner.

MATERIALS

Aceclofenac and Soluplus were generous gifts from Ultratech Pharmaceutical, India, and BASF Chemical Co. Mumbai, India, respectively. Acetone (SD Fine Chemicals, Mumbai) was used in the study. The chemical structures of drug and polymer are shown in Fig. 1.

METHODS

Estimation of $\chi_{d\text{-}p}$ Using Solubility Parameter

The interaction parameter, $\chi_{d\text{-}p}$, was estimated by using Hildebrand and Scott method.

$$\chi_{d-p} = \frac{V\left(\delta_{drug} - \delta_{polymer}\right)^2}{RT} \tag{5}$$

Here, V the drug molar volume, and δ_i denotes the solubility parameter of component i. Solubility parameter, also defined as the square root of the cohesive energy density E_{coh}, is estimated as per the following equation:

$$\delta^2 = \delta^2_d + \delta^2_p + \delta^2_h \tag{6}$$

where δ_d, δ_p, and δ_h denote solubility parameter components representing individual contribution from dispersion
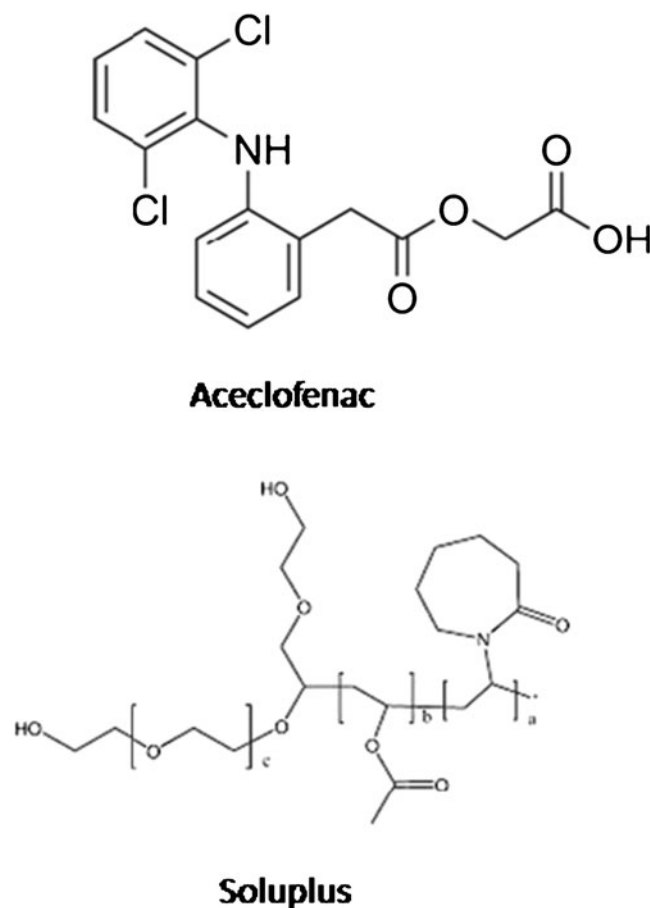

Fig. 1. Chemical structure of aceclofenac and Soluplus

forces, polar forces, and hydrogen bonding forces, respectively. The values of δ_d, δ_p, and δ_h were estimated indirectly using Van Krevelen group contribution method, as per the following equations:

$$\delta_d = \frac{\sum F_{di}}{V} \quad \delta_p = \frac{\sqrt{\sum F_{pi}^2}}{V} \quad \delta_h = \sqrt{\frac{\sum E_{hi}}{V}} \tag{7}$$

where F_{di}, F_{pi}, and E_{hi} are the group contributions at 25°C, as reported in literature for the occasionally occurring structural components in organic molecules (18). Theoretical estimation of molar volume V was done by employing group contribution values for different groups as suggested by Fedor (19).

Determination of $\chi_{d\text{-}p}$ Using Melting Point Depression

DSC Q10 V9.9, Build 303 model (Universal V4.5A TA instruments), was used for the purpose. The instrument was calibrated in standard mode for temperature using indium. Nitrogen, 45 ml/min, served as the purge gas. Physical mixtures were prepared by geometric mixing at concentrations of 5, 10, 15, 20, 25, and 30 wt% Soluplus with aceclofenac. Samples, sealed non-hermetically in aluminum pans, were heated to 170°C at scan rate of 5°C/min. The onset of melting was taken as the extrapolated onset of the bulk melting endotherm.

Construction of Phase Diagram

Phase diagram for aceclofenac–Soluplus binary system was constructed based on two different approaches:

Approach 1. Subjecting drug–polymer mixtures with different drug loading to thermal analysis led to depression in drug melting point. Substituting this value in Eq. 8 allowed estimation of $\chi_{d\text{-}p}$ at different temperatures.

$$\ln\varphi_d + (1-1/m)\varphi_p + \chi_{d\text{-}p}\varphi_p^2 = \frac{\Delta H}{R}\left(1/T_m^o - 1/T_m\right) \quad (8)$$

where T_m and T_m^o are the melting points of the crystalline drug in the drug/polymer mixture and of the pure drug, respectively; ΔH is the heat of fusion of pure drug. Subsequently, linear fit of $\chi_{d\text{-}p}$ vs. $1/T$ yielded values of constants A and B as per Eq. 3 (27).

Approach 2. The solubility parameter method gave us the drug–polymer interaction parameter at 25°C. On the other hand, melting point depression data yielded interaction parameter at temperature near the melting point of the drug. On the basis of Eq. 3, which hypothesizes a linear relationship between temperature and interaction parameter, it was possible to interpolate the value of interaction parameter at various temperatures (28).

To summarize, while approach 1 uses relationship of interaction parameter vs. temperature based solely on melting point depression data, approach 2 incorporates additional contribution from solubility parameter into this relationship.

By substituting $\chi_{d\text{-}p}$ values calculated at different temperatures into Eq. 1, it was possible to estimate the change in ΔG_{mix} as a function of drug composition at the corresponding temperature. Combination of Eqs. 3 and 4 allowed expression of spinodal phase separation curve ($T-\varphi$) as a simplified equation ([27]; Eq. 9).

$$T_s = \frac{2B}{1/\varphi_d + \left(1/(m(1-\varphi_d))\right) - 2A} \quad (9)$$

The spinodal curve representing boundary line between the unstable and metastable region for the particular drug–polymer system was obtained by plotting these compositions vs. temperature.

Estimation of Drug Solubility. The solubility of crystalline drug in polymer has been proposed to be estimated by an extension of the solubility theory. As per the approach, free energy of fusion of the crystalline solid is added to the partial molal free energy of dilution of amorphous polymer. The resulting sum must equal to zero at equilibrium (17). Hence, Eq. 8 was used for the estimation of drug solubility at pharmaceutical relevant temperatures.

Estimation of T_g Curve. The glass transition of a drug–polymer binary system (T_{gmix}) was estimated as weighted average of T_gs of pure components using Gordon–Taylor equation (30) as follows:

$$T_{gmix} = \frac{\{(w_1 T_{g1}) + (K\,w_2 T_{g2})\}}{(w_1 + K\,w_2)} \quad K = \rho_1 T_{g1}/\rho_2 T_{g2} \quad (10)$$

where w_i, T_{g_i}, and ρ_i are respectively the weight fraction, the glass transition temperature, and density of component i.

Preparation of Solid Dispersions

On the basis of phase diagram, two compositions were identified corresponding to two different regions in phase diagram. Hence, SDs containing 0.20 or 0.80 weight fraction of aceclofenac was prepared by solvent evaporation method. Weighed amount of drug was dissolved in a solution of Soluplus in acetone. The solvent was removed by evaporation under vacuum at 40°C. Freshly prepared SD was pulverized and sifted through sieve no. 44 and characterized suitably. Select batches of SD were stored at ambient conditions (RH ~40% at RT) to perform 6 months aging studies.

Validation of the Phase Diagram

Powder X-Ray Diffraction. The powder samples were analyzed using X-ray diffractometer (X'pert pro PANnalytical, Netherland) under the following condition: Ni-filtered Cu Kα radiation, voltage 40 kV, current 40 mA, 2θ range of 5–50°C, and scan rate 2°/min.

Differential Scanning Calorimetry. Instrument details are same as above. Powder samples, sealed non-hermetically in aluminum pans, were heated to 170°C at scan rate of 10°C/min.

In Vitro Dissolution. Dissolution studies of powder samples were performed using USP type 2 dissolution apparatus (Harrison's HDA/D). Hundred milligrams of aceclofenac (or an equivalent amount in case of SD) was added to 900 ml phosphate buffer pH 7.4 at 37±0.5°C and stirred at 50 rpm. Aliquot of 5 ml was withdrawn regularly with volume replacement. Sample were suitably diluted and the absorbance measured (λ_{max} 275 nm) using Systronic 2203, double beam UV spectrophotometer.

All the dissolution profiles were evaluated by two fundamental parameters, i.e., dissolution efficiency and dissolved percentage. Dissolution efficiency (DE) is a model independent parameter and is employed to compare the dissolution profiles of two different formulations (31). It is calculated according to the formula:

$$DE_T = \frac{\int_0^T y_t \cdot dt}{y_{100} \cdot T} \quad (11)$$

where DE_T is DE at time T, y_t is percent of drug dissolved at any time t, y_{100} denotes 100% dissolution, and the integral represents the area under dissolution curve between time zero and T. Dissolved percentage represents percentage drug contents dissolved in dissolution medium at time t.

RESULTS AND DISCUSSION

Estimation of $\chi_{d\text{-}p}$ Using Solubility Parameter

The solubility parameter values for aceclofenac and Soluplus were calculated to be 21.79 and 26.40 MPa$^{1/2}$, respectively. For the estimation of solubility parameter for
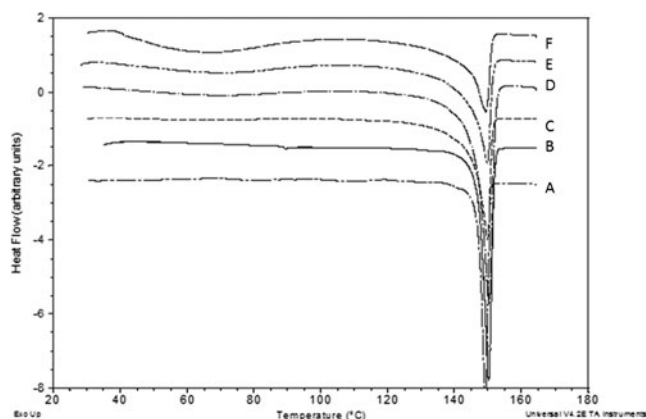
Fig. 2. Heating curves for drug aceclofenac and its physical mixture with different proportion of polymer. *A* Aceclofenac, physical mixtures containing *B* 0.95, *C* 0.90, *D* 0.85, *E* 0.80, and *F* 0.75 weight fraction of drug

Soluplus, solubility parameter of three monomers (−vinyl caprolactum, −vinyl acetate, and −ethylene glycol) and of chain end groups of Soluplus were calculated separately and the total solubility parameter was estimated by the number of average solubility parameter of these three monomers and end chain group (detailed calculations are included in Annexure I). It been reported that components with similar solubility parameters (~7 MPa$^{1/2}$) are more likely to be miscible, whereas compounds with solubility parameters differing by more than 10 MPa$^{1/2}$ are most probably immiscible (32). In the present case, the difference between the solubility parameter of drug and polymer was small (~5 MPa$^{1/2}$), which suggests mutual miscibility of the drug and polymer. The value of χ_{d-p} at 25°C was found to be 2.348 using Eq. 5.

Estimation of χ_{d-p} Using Melting Point Depression

Figure 2 represents heating curves for physical mixture of drug and polymer containing varying relative fraction of drug and polymer. Heating curve of pure drug shows an endotherm at 149.3°C, attributed to the drug melting. A comparison of heating curves for physical mixtures containing different fraction of polymer shows that as the polymer fraction in a physical mixture is increased, the onset temperature as well as the heat of fusion is gradually reduced. The depression in the melting point of drug in the binary mixture is considered to be indicative of mutual mixing between two components at the higher temperatures (11).

Construction of Free Energy and Temperature–Composition Phase Diagram

Approach 1. The onset temperature of the drug melting endotherm was used for plotting $(1/T_m - 1/T_m^o) \times (\Delta H_{fus}/-R)-$

$\ln(\emptyset_{drug}) - (1-1/m)\emptyset_{polymer}$ *versus* $\emptyset_{polymer}^2$ (the properties of drug and polymer used in estimation are listed in Table I). The slope of the straight line, found to be +0.66 in the present case, gave the value of χ_{d-p} at the melting point of drug. It is known that a negative or slightly positive value of interaction parameter is indicative of adhesive interaction between the drug and polymer and suggest mixing. The lower value of interaction parameter represents a miscible system and suggests some degree of favorable interactions between drug and polymer.

A plot of interaction parameter *versus* $1/T$ was linear ($r^2=0.85$) across the experimental composition. The values of *A* and *B* were calculated to be −5.565 and 2495, respectively.

Approach 2. The value of χ_{d-p} using solubility parameter at 25°C and melting point depression method at melting point of drug was found to be 2.348 and +0.66, respectively. By combining the two sets of values of interaction parameter, Eq. 3 was solved as

$$\chi_{d-p} = -3.386 + \frac{1709}{T}$$

By substituting value of χ_{d-p} in Eq. 1, it was possible estimate ΔG_{mix} for varying relative fraction of drug and polymer at the corresponding temperature. Results from such an estimation are plotted in Fig. 3, for the drug–polymer binary system for a range of temperatures. As mentioned earlier, the ΔG_{mix} for a composition can be either negative (indicating spontaneous mixing) or positive (indicating unfavorable mixing). In addition, spontaneous small fluctuations may eventually lead to phase separation in a binary system when a system lowers its free energy by separating into two phases. It is expected that as long as ΔG_{mix} curve is concave up, the phase separation would actually lead to increase in free energy of the system. Hence, "concave up" gives the criteria for the stability of one-phase system while the reverse is expected to be applicable to the "concave down" free energy curve.

By incorporating the temperature dependence of χ_{d-p}, and using Eq. 4, the spinodal curve was obtained using two different approaches (Fig. 4). It is evident that there was no significant difference between the curves obtained using the two different approaches. The spinodal curve provides an overall picture of thermal stability and helps to determine whether the mixture is locally stable or experiences spontaneous phase separation upon temperature or composition change. In the regions representing drug–polymer compositions below this curve, a single-phase homogeneously mixed binary system is expected to spontaneously phase separate into two phases, i.e., drug-rich phase and polymer-rich phase at the corresponding temperature. On the other hand, in the region representing composition–temperatures above the curve, the single-phase binary system is expected to remain unchanged due to the resulting increase in free energy of the system associated with such phase separation. Thus, at elevated temperature, homogeneous mixtures are generated, that

Table I. Physical Properties Used with Melting Point Depression Data to Calculate the F–H Interaction Parameter

Compound	M_w (g/mol)	Density (g/cm³)	Molecular volume (cm³/mol)	ΔH_{fusion} (kJ/mol)
Aceclofenac	354.17	1.455	243.42	51.11
Soluplus	115,000	0.99	116,161.62	–

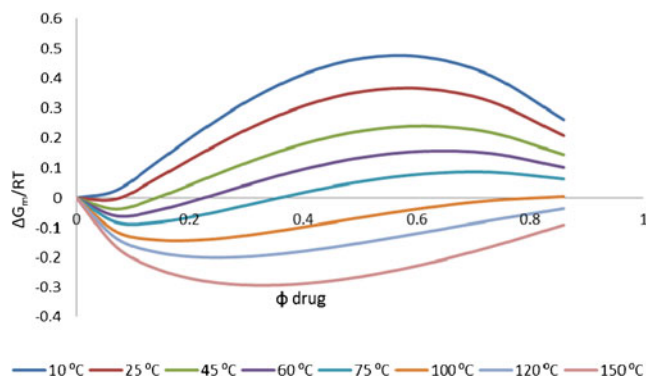**Fig. 3.** Plot of $\Delta G_{mix}/RT$ as function of drug volume fraction for aceclofenac–Soluplus binary system at different temperatures

Fig. 5. The XRD pattern of *A* aceclofenac. *B* SD containing 0.80 weight fraction drug. *C* SD containing 0.20 weight fraction drug, freshly prepared. *D* SD containing 0.20 weight fraction drug, aged

are thermodynamically stable at all drug–polymer compositions. The figure reveals that the phase diagram for aceclofenac–Soluplus system is skewed/asymmetric to the left, with the critical composition at an extreme low concentration of polymer. This indicates that a high concentration of polymer is required to ensure that any phase separation is eventually prevented. The temperature–composition phase diagram provides an estimate of the saturation limit of amorphous drug loading in a polymer at different temperatures.

Incorporation of solubility curve and the calculated T_g line in the drug–polymer phase diagram give us a working diagram of practical relevance. The region of phase diagram below T_g line and above the solubility curve are expected to be "safe zones," within which small drug concentration or temperature fluctuations may not destabilize the system. In the region below solubility and T_g curve while above miscibility curve, the driving force for destabilization of the system is expected to be the crystallization of supersaturated drug (14,26). The SD containing 0.20 weight fraction drug seem to belong to the particular region of the phase diagram and is expected to be stabilized thermodynamically (below miscibility) and kinetically (low-molecular mobility below T_g). The SD containing 0.80 weight fraction drug represents the high drug loading region well below the
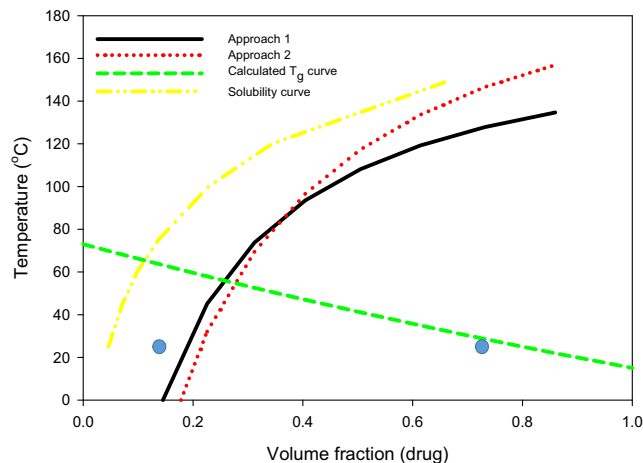
miscibility curve and spontaneous crystallization is expected in the absence of any significant energy barrier.

While a comprehensive examination of solid dispersion through phase diagrams defined by temperature and drug loading are helpful, it is to acknowledge the fact that the change from higher *G* state to lower *G* state maybe sometimes kinetically hindered or maybe occurring in the time scale too long. In such, kinetically hindered transitions, phase diagrams are still useful tools in that they at least provide constraints and driving forces on transitions (33). Though the phase boundary may not be precise and may deviate for practical systems, these estimations may still be useful at the early stage of understanding the system behavior.

Validation of Phase Diagram

In order to qualitatively validate the binary phase diagram, the two drug–polymer compositions were selected, one from each side of the estimated miscibility curve. The SDs of

Fig. 4. Temperature–composition phase diagram of aceclofenac and Soluplus system showing spinodal curves estimated using two different approaches (see text for details), T_g curve calculated as per Gordon–Taylor equation, and the solubility curve. The positions of two select compositions with respect to room temperature are marked as points on the phase diagram
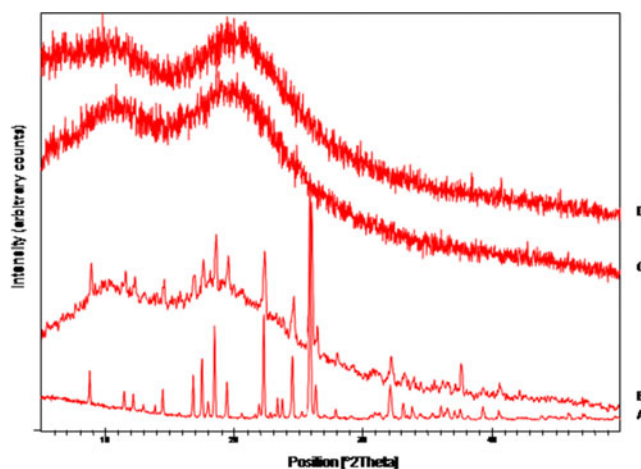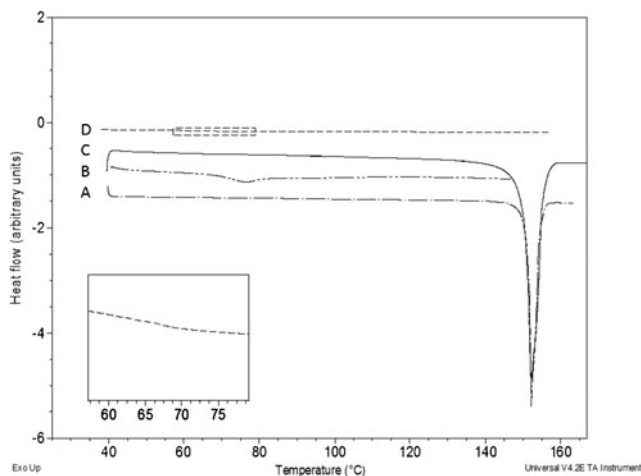

Fig. 6. DSC heating curves for *A* aceclofenac, *B* Soluplus, *C* SD containing 0.80 weight fraction drug, and *D* SD containing 0.20 weight fraction drug (*inset* shows expanded region in the heating curve)
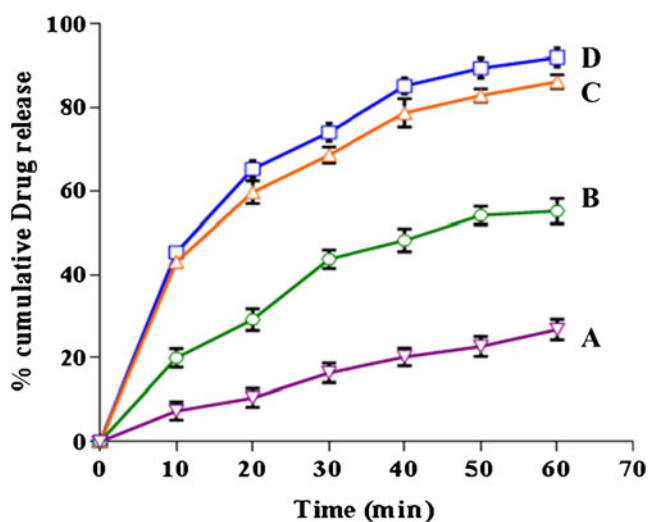
Fig. 7. Dissolution profiles of *A* aceclofenac, *B* freshly prepared SD containing 0.80 weight fraction drug, *C* SD containing 0.20 weight fraction drug, aged for 6 months, *D* freshly prepared SD containing 0.20 weight fraction drug (*n*=3)

the particular drug–polymer compositions were prepared and were characterized fresh as well as after storage at ambient conditions for 6 months.

Powder X-Ray Diffraction. Fresh SD containing 0.20 weight fraction drug exhibited a broad halo in the X-ray diffraction (XRD) pattern (Fig. 5), which suggest the amorphous nature of the drug in the dispersion. On the other hand, XRD pattern of the SD containing 0.80 weight fraction drug exhibited the presence of sharp diffraction peaks at 8.89, 14.58, 16.91, 17.62, 18.63, 19.53, 22.39, 24.62, 26.09, and 32.21 °2θ, which correspond to the characteristic peaks for crystalline aceclofenac. The distinct diffraction peaks in the SD are indicative of the presence of drug in the crystalline form in the SD, though a small halo characteristic of the XRD pattern of the polymer is also evident. As the freshly prepared SD containing 0.80 weight fraction drug was itself found to contain drug in the crystalline form, it was not subjected to aging studies. The XRD pattern for 6-month aged SD containing 0.20 weight fraction drug exhibited a broad halo, and there was no discernible difference between the XRD patterns of fresh and aged SD, suggesting that the drug was retained in the amorphous form in the SD.

Differential Scanning Calorimetry. Differential scanning calorimetry (DSC) is commonly employed to determine the number of amorphous phases present in systems containing more than one component. The presence of a single amorphous phase, where molecules of the different components present are mixed "at the molecular level," is commonly inferred from the presence of a single T_g. In contrast, the presence of more than one T_g is indicative of the presence of

more than one amorphous phase (34). SD containing 0.20 weight fraction drug exhibited a single thermal event, T_g at ~66°C (Fig. 6). Interestingly, the T_g value was found to be in between the T_gs of the pure components (T_g for polymer ~73°C; reported T_g of amorphous aceclofenac ~15°C, predicted T_g as per the Gordon–Taylor equation 63°C). This transition was lower than the T_g of the polymer, suggesting that the drug is present in amorphous form in the polymer.

The SD containing 0.80 weight fraction drug showed a sharp endothermic peak at melting point of drug, which suggests presence of drug in the crystalline form. The results are consistent with XRD observation. It is expected that the SD containing 0.80 weight fraction drug may consist of a crystalline drug phase (evident from the sharp melting point) and a minor phase wherein small amount of the drug is retained amorphous due to polymer. Instrument sensitivity may be a limiting factor for the lack of evidence for the minor phase.

In Vitro Dissolution. Figure 7 depicts the dissolution profiles of drug and SDs and the dissolution efficiencies of different samples are compiled in Table II. Dissolution from the pure aceclofenac was found to be slow as revealed by the DP_{10}~7.38% and DE_{60}~0.26. Interestingly, the SD containing 0.20 weight fraction drug showed significant enhancement in dissolution rate (DP_{10}~45.45% and DE_{60}~0.92). The increase in DEs may be attributed to the presence of the drug in the amorphous form, as suggested by XRD and DSC results (Figs. 5 and 6). Storage of the SD under ambient conditions for 6 months did not cause an appreciable change in the dissolution behavior of the SD (DP_{10}~43.14% and DE_{60}~0.86). The results are consistent with XRD observations, which suggest that higher proportion of polymer retained the drug in amorphous form over a period of 6 months. Combination of information from phase diagram and thermal analysis suggests that the aging temperature which SD was subjected to was well below its glass transition temperature, implying stable system.

In contrast, SD containing 0.80 weight fraction drug showed a moderate enhancement in dissolution rate of drug (DP_{10}~20.05% and DE_{60}~0.55). Though XRD and DSC results suggested the existence of drug in the crystalline form in the SD (Figs. 5 and 6), the small increase in DE is indicative of the presence of minor amount of drug in the amorphous form. The findings again suggest that the SD consisting of 0.80 weight fraction drug may be considered to consist of at least two phases.

Various factors have been proposed to account for the increased dissolution of drug in SD as compared to that of the drug alone. These include decreased particle size of drug, specific form of drug in the SDs, increase in the drug wettability, and prevention of drug aggregation/crystallization by polymer due to increase in viscosity (35). The characterization of the SDs prepared in the present study suggests that the drug was present in the amorphous form in the SDs, which could be

Table II. Dissolution Characteristics of Aceclofenac and Its Solid Dispersions Using Phosphate Buffer pH 7.4 at 37°C (mean±SD; *n*=3)

Sample	DP_{10}	DE_{10} (%)	DE_{60} (%)
Aceclofenac	7.38±2.18	7.38±2.18	26.85±2.49
SD containing 0.20 weight fraction drug-fresh	45.45±1.13	45.45±1.13	92.10±2.25
SD containing 0.80 weight fraction drug-fresh	20.05±2.24	20.05±2.24	55.20±3.0
SD containing 0.20 weight fraction drug-aged	43.14±1.53	43.14±1.53	86.33±1.65

considered as an important factor in enhancement the dissolution rate. It is well established that amorphous drug represents the most ideal case for fast drug dissolution (4).

CONCLUSION

Prediction of behavior of drug–polymer binary system is of practical significance in view of potential advantage of such a system in improving solubility of sparingly soluble drugs. In the present study, temperature–composition phase diagram of model system consisting of aceclofenac and Soluplus was generated on the basis of the Flory–Huggins theory. Estimation of binary drug–polymer interaction parameter suggested mutual miscibility of the drug and polymer. Experimental evidence also revealed that the drug was retained in the amorphous form in the presence of higher fraction of polymer. The study shows that it is possible to employ such an estimation as a preliminary tool to estimate behavior of a binary system.

ANNEXURE I

Calculation of solubility parameter for aceclofenac and Soluplus

1. Aceclofenac ($C_{16}H_{13}Cl_2NO_4$)

Structural groups	No.	F_{di} $(MJ/m^3)^{1/2}mol^{-1}$	F_{pi}^2 $(MJ/m^3)^{1/2}mol^{-1}$	E_{hi} J/mol	V m^3/mol
-Phenyl	2	2860	24,200	0	142.8
-Cl	2	900	500,000	800	48.0
-NH	1	160	44,100	3100	4.5
-COOH	1	530	176,400	10,000	28.5
-CH₂	2	540	0	0	32.2
-COO-	1	390	240,100	7000	18
Σ		5380	984,800	20,900	274.0

$\delta_{drug}=21.79$

2. Soluplus
A graft copolymer comprising of polyvinyl caprolactum–polyvinyl acetate-polyethylene glycolin ratio proposed as m: n: l =0.3: 0.13: 0.57

(a) $(C_4H_6O_2)_m$

Structural groups	No.	F_{di} $(MJ/m^3)^{1/2}mol^{-1}$	F_{pi}^2 $(MJ/m^3)^{1/2}mol^{-1}$	E_{hi} J/mol	V m^3/mol
1 CH₃	311	130,620	0	0	10,418.5
1 CH₂	311	83,970	0	0	5007.1
1 CH	311	24,880	0	0	−311.0
1 COOH	311	121,290	2.32E+10	2,177,000	5598.0
Σ		360,760	2.32E+10	2,177,000	20,712.6

$\delta(C_4H_6O_2)_m=21.50$

(b) $(C_2H_4O)_n$

Structural groups	No.	F_{di} $(MJ/m^3)^{1/2}mol^{-1}$	F_{pi}^2 $(MJ/m^3)^{1/2}mol^{-1}$	E_{hi} J/mol	V m^3/mol
2 CH₂	270	72,900	0	0	4347
1 O	135	13,500	2.92E+09	405,000	513
Σ		86,400	2.92E+09	405,000	4860

$\delta(C_2H_4O)_n=22.86$

(c) $(C_8H_{13}NO)_l$

Structural groups	No.	F_{di} $(MJ/m^3)^{1/2} mol^{-1}$	F_{pi}^2 $(MJ/m^3)^{1/2} mol^{-1}$	E_{hi} J/mol	V m^3/mol
6-CH2-	3552	959,040	0	0	57,187.2
1-CH-	592	47,360	0	0	−592.0
1-N-	592	11,840	2.24E+11	2,960,000	−5328.0
1 C=O	592	11,840	2.24E+11	2,960,000	−5328.0
1-RING	592	112,480	0	0	9472.0
Σ		1,142,560	4.49E+11	5,920,000	55,411.2

$\delta(C_8H_{13}NO)_l = 23.84$

(d) Chain end 1

Structural groups	No.	F_{di} $(MJ/m^3)^{1/2} mol^{-1}$	F_{pi}^2 $(MJ/m^3)^{1/2} mol^{-1}$	E_{hi} J/mol	V m^3/mol
OH	1	210	250,000	20,000	10.0
CH2	3	810	0	0	48.3
O	2	200	640,000	6000	7.6
CH	1	80	0	0	−1.0
Σ		1300	890,000	26,000	64.9

$\delta_{(Chain\ end\ 1)} = 29.23$

(e) Chain end 2

Structural groups	No.	F_{di} $(MJ/m^3)^{1/2} mol^{-1}$	F_{pi}^2 $(MJ/m^3)^{1/2} mol^{-1}$	E_{hi} J/mol	V m^3/mol
CH_2	2	270	0	0	16.1
OH	1	210	250,000	20,000	10.0
Σ		480	250,000	20,000	26.1

$\delta(Chain\ end\ 2) = 34.58$
Combination of a-e, as calculated above, gives the value of $\delta_{polymer} = 26.41$

REFERENCES

1. Lipinski CA, Lombard F, Dominy BW, Feeney PJ. Experimental and computational approaches to estimate solubility and permeability in drug discovery and development settings. Adv Drug Deliv Rev. 2001;46:3–26.
2. Che E, Zheng X, Sun C, Chang D, Jiang T, Wang S. Drug nanocrystals: a state of art formulation strategy for preparing the poorly water-soluble drugs. Asian J Pharm Sci. 2012;7(2):85–95.
3. Kaushal AM, Gupta P, Bansal AK. Amorphous drug delivery systems: molecular aspects, design and performance. Crit Rev Ther Drug Carrier Syst. 2004;21:133–93.
4. Hancock BC, Zografi G. Characteristics and significance of the amorphous state in pharmaceutical systems. J Pharm Sci. 1997;86:1–12.
5. Yu L. Amorphous pharmaceutical solids: preparation, characterization and stabilization. Adv Drug Deliv Rev. 2001;48:27–42.
6. Chiou WL, Riegelman S. Pharmaceutical applications of solid dispersion systems. J Pharm Sci. 1971;60(9):1281–302.
7. Leuner C, Dressman J. Improving drug solubility for oral delivery using solid dispersions. Eur J Pharm Biopharm. 2000;50:47–60.
8. Serajuddin ATM. Solid dispersion of poorly water-soluble drugs: early promises, subsequent problems, and recent breakthroughs. J Pharm Sci. 1999;88:1058–66.
9. Craig DQM. The mechanisms of drug release from solid dispersions in water-soluble polymers. Int J Pharm. 2002;231:131–44.
10. Teja SB, Patil SP, Shete G, Patel S, Bansal AK. Drug-excipient behavior in polymeric amorphous solid dispersions. J Exp Food Chem. 2013;4(3):70–94.
11. Baird JA, Taylor LS. Evaluation of amorphous solid dispersion properties using thermal analysis techniques. Adv Drug Deliv Rev. 2012;64(5):396–421.
12. Kakumanu VK, Bansal AK. Enthalpy relaxation studies of celecoxib amorphous mixtures. Pharm Res. 2002;19:1873–8.
13. Pajula K, Taskinen M, Lehto V, Ketolainen J, Korhonen O. Predicting the formation and stability of amorphous small molecule binary mixtures from computationally determined Flory-Huggins interaction parameter and phase diagram. Mol Pharm. 2010;7(3):795–804.
14. Qian F, Huang J, Hussain M. Drug-polymer solubility and miscibility: stability consideration and practical challenges in amorphous solid dispersion development. J Pharm Sci. 2010;99:2941–7.
15. Flory PJ. Principles of polymer chemistry. Ithaca: Cornell University Press; 1953.
16. Huggins ML. Thermodynamic properties of solutions of long-chain compounds. Ann N Y Acad Sci. 1942;43(1):1–32.
17. Hildebrand J, Scott R. Solubility of non-electrolytes. 3rd ed. New York: Reinhold; 1950.
18. Fedors RF. A method for estimating both the solubility parameters and molar volumes of liquids. Polym Eng Sci. 1974;14:147–54.
19. Van Krevelen DW, TeNijenhuis K. Properties of polymers. 4th ed. Oxford: Elsevier Scientific Publication; 2009.
20. Thakral S, Thakral NK. Prediction of Drug–polymer miscibility through the use of solubility parameter based Flory–Huggins interaction parameter and the experimental validation: PEG as model polymer. J Pharm Sci. 2013;7(102):2254–63.
21. Nishi T, Wang T. Melting-point depression and kinetic effects of cooling on crystallization in poly (vinylidene fluoride) poly(methyl methacrylate) mixtures. Macromolecules. 1975;8:909–15.

22. Marsac P, Shamblin S, Taylor LS. Theoretical and practical approaches for prediction of drug-polymer miscibility and solubility. Pharm Res. 2006;23:2417–26.

23. Marsac P, Li T, Taylor LS. Estimation of drug-polymer miscibility and solubility in amorphous solid dispersions using experimentally determined interaction parameters. Pharm Res. 2009;26:139–51.

24. Koningsveld R, Solc K. Liquid-liquid phase-separation in multicomponent polymer systems: influence of molar-mass distribution on shadow curve and phase-volume ratio. Collect Czech Chem Commun. 1993;58:2305–20.

25. Solc K, Koningsveld R. Liquid-liquid phase separation in multicomponent polymer systems, blends of two polydisperse polymers. Collect Czech Chem Commun. 1995;60:1689–718.

26. Tian Y, Booth J, Meehan E, Jones DS, Li S, Andrews GP. Construction of drug–polymer thermodynamic phase diagrams using Flory–Huggins interaction theory: identifying the relevance of temperature and drug weight fraction to phase separation within solid dispersions. Mol Pharm. 2012;10(1):236–48.

27. Lin D, Huang YA. Thermal analysis method to predict the complete phase diagram of drug-polymer solid dispersions. Int J Pharm. 2010;399:109–15.

28. Zhao Y, Inbar P, Chokshi H, Malick AW, Choi D. Prediction of the thermal phase diagram of amorphous solid dispersions by Flory–Huggins theory. J Pharm Sci. 2011;100:3196–207.

29. Tian B, Wang X, Zhang Y, Zhang K, Tang X. Theoretical prediction of a phase diagram of solid dispersion. Pharm Res. 2014: 1–12.

30. Gordon M, Taylor JS. Ideal copolymers and the second-order transitions of synthetic rubbers. I. non-crystalline copolymers. J Appl Chem. 1952;2(9):493–500.

31. Khan KA. The concept of dissolution efficiency. J Pharm Pharmacol. 1975;27:48–9.

32. Forster A, Hempenstall J, Tucker I, Rades T. Selection of excipients for melt extrusion with two poorly water-soluble drugs by solubility parameter calculation and thermal analysis. Int J Pharm. 2001;226:147–61.

33. Martin SC. Phase transitions in aqueous atmospheric particles. Chem Rev. 2000;100:3403–53.

34. Olabisi O, Robeson L, Shaw M. Polymer-polymer miscibility. San Diego: Academic Press, Inc.; 1979.

35. Tantishaiyakul V, Kaewnopparat N, Ingkatawornwong S. Properties of solid dispersions of piroxicam in polyvinylpyrrolidone. Int J Pharm. 1999;181(2):143–51.